A Graph Search Approach for Automated Scientific Planetary Moon Tour Design with Mission Constraints

Francesco Persenico(1), Fabrizio Maccari(1), Michèle Lavagna(1)

(1)*Politecnico di Milano*
Milano, Italy
Email: fabrizio.maccari@polimi.it

Abstract **– Planetary Moon Tours represent a complex mission analysis problem, requiring the optimization of high-dimensional and mixed-integer design spaces. This work extends recent automated trajectory design approaches beyond single-target moon orbit insertion by integrating mission constraints and scientific objectives directly into the optimization process.**

The proposed method combines trajectory optimization and feasibility assessment within a graph-based framework. It considers constraints such as surface-coverage requirements and flyby altitude limits, while remaining flexible enough to include additional mission and operational requirements. The design space is discretized using resonant and non-resonant transfers, VILTs, COT sequences, and unpowered flybys, all mapped on each moon's V-Infinity Globe.

The pipeline first builds and optimizes single-moon phases using a Keplerian patched-conics model. A scalar cost function combining ΔV, Time of Flight, and flyby surface coverage enables the use of Dijkstra's algorithm to identify optimal flyby sequences. As a preliminary extension toward multi-moon Tour design, these single-moon solutions are then connected through inter-moon Lambert arcs within an external graph structure, explored using an IG-UCS algorithm.

The approach is tested in the Saturnian system, demonstrating its ability to autonomously generate high-coverage, low-ΔV flyby sequences and providing an initial feasibility assessment for assembling multi-moon tours.

I. INTRODUCTION

Planetary moon exploration in the outer Solar System is one of the most attractive and demanding areas of mission analysis. Missions such as Galileo and Cassini demonstrated the scientific relevance of giant-planet satellites, especially icy moons potentially hosting subsurface oceans and active geophysical processes [1]. This interest has motivated more recent missions such as JUICE and Europa Clipper, based on long-duration operations and repeated close flybys in multi-moon systems [2].

From an astrodynamics perspective, these missions are difficult because the spacecraft must control its energy and encounter geometry over long time spans, while satisfying strict propellant, time, navigation, altitude, communication, and scientific constraints. Direct capture around a target moon is often too expensive in terms of ΔV, especially for moons deep inside the planet's gravity well. For this reason, Moon Tours are commonly adopted: sequences of planet-centred arcs and multiple gravity assists that progressively reshape the spacecraft orbit until favourable encounter conditions are reached. In this work, the tour is not treated as an Endgame problem aimed at final orbital insertion, but as a flyby-driven mission in which the objective is to maximize science return through repeated encounters while minimizing ΔV and Time of Flight (*ToF*).

Moon Tour design is particularly challenging because moon systems generate dense and highly combinatorial design spaces. Orbital and synodic periods are short, transfer opportunities recur frequently, and discrete choices, such as the next moon or transfer type, are strongly coupled with continuous variables, such as encounter timing, v∞ direction, flyby altitude, and possible deep-space manoeuvres. Classical global optimization strategies can therefore become inefficient unless the problem is carefully structured. This motivates the use of automated search pipelines able to generate high-quality initial guesses under mission-related constraints, which can later be refined in higher-fidelity models.

The state of the art provides several modelling tools and transfer strategies to structure the Moon Tour design space. In this work, two aspects are especially relevant: a representation tool is needed to describe and connect feasible encounter states, while a set of efficient transfer families is required to define the admissible transitions between them. The V-Infinity Globe, shown in Figure 1, is especially relevant because it maps each encounter through v∞, pump angle (α), crank angle (κ), and encounter longitude, allowing the effect of a gravity assist to be represented as a rotation of the v∞ vector [3]. It is particularly suitable for same-body flyby sequences and was used in the design of Cassini's extended mission. The Globe exploits two angles: the pump angle, defined between the v∞ vector and the moon's velocity vector, and the crank angle, measuring the out-of-plane component of the v∞ vector with respect to the orbital plane of the

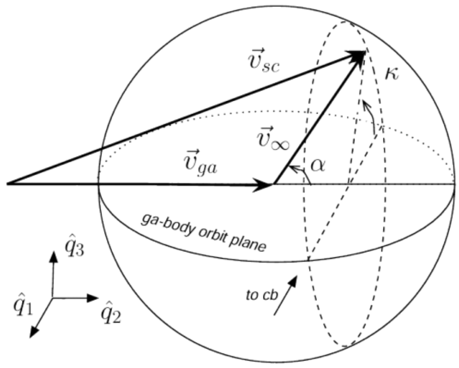

Figure 1: V-Infinity Globe [3].

moon.

Tisserand and Tisserand-Poincaré graphs offer useful complementary representations too, especially for visualising energy levels, low-energy regions, and ballistic capture opportunities in planar models [4]. More advanced CR3BP-based tools, such as the Flyby Map and the CWIC hybrid model, improve the description of close encounters but introduce additional modelling and computational complexity [5].

The main ballistic transfer families considered are resonant transfers, non-resonant transfers, Cranking Over the Top (COT) sequences, and cyclers. Resonant and non-resonant transfers are useful same-body building blocks because, under circular and coplanar moon-orbit assumptions, they can be described through phase-independent relations [6]. COT sequences are especially important for this work because repeated resonant flybys can change the crank angle while also improving surface coverage, which directly supports science-driven tour design [7]. Cyclers offer repeatable low-propellant motion between moons, but they are less suitable here because they typically revisit only two or three bodies and may not improve surface coverage effectively for tidally locked moons.

Powered transfer strategies are needed to change the $v\infty$ level with respect to the same moon. V-Infinity Leveraging Transfers (VILTs) use a deep-space manoeuvre far from the flyby body to modify encounter energy efficiently in a Keplerian patched-conics model [8]. Their main advantage is low computational cost, making them suitable for large-scale automated searches. Tisserand Leveraging Transfers extend this concept to the CR3BP and can exploit low-energy dynamics, but require Flyby Maps and partial numerical integration, increasing complexity [9]. Fully multibody techniques and patched periodic orbits can produce very low-ΔV solutions, but they are computationally expensive and often require predefined resonance structures or large trajectory databases.

For optimization, classical genetic algorithms and exhaustive tree searches are not ideal because of the size of the Moon Tour design space. Beam search has proven effective in large astrodynamics combinatorial problems, such as GTOC, by pruning less promising branches during the search [10,11]. More recently, graph-based methods have become attractive because they can represent large trajectory spaces while allowing constraints and cost functions to be embedded directly in the search [12,13].

Accordingly, the core contribution of this work is the automated construction and optimization of constrained single-moon flyby phases. These phases are built from resonant transfers, non-resonant transfers, COT sequences, VILTs, and unpowered flybys mapped on the V-Infinity Globe, and are optimized through Dijkstra's algorithm [14]. A preliminary extension toward multi-moon Tour design is then investigated through an external phase-dependent graph, where optimized single-moon phases are connected by inter-moon Lambert arcs and explored with an Implicit Graph – Uniform Cost Search (IG-UCS) algorithm. This second layer provides an initial feasibility assessment for assembling multi-moon sequences, while leaving further refinement of the inter-moon patching strategy to future work.

II. Design Space Definition

The Moon Tour design space is defined by selecting a set of elementary transfers that can be used as building blocks and then patching them together through unpowered flybys. The trajectory model adopted at this stage is the 0-Sphere Of Influence (SOI) patched-conics approximation, which allows each transfer to be represented through its incoming and outgoing encounter conditions on the V-Infinity Globe. In this way, the continuous trajectory design problem is converted into a discrete combinatorial search problem, where each node or edge of the graph corresponds to a feasible encounter state or transfer opportunity.

The building blocks included in the database are the following:

- **Resonant Transfers**: trajectories connecting two gravity assists occurring at the same position on the moon's orbit around the primary. They are identified by the N:M resonance ratio, where N is the number of moon revolutions and M is the number of spacecraft revolutions around the primary between two consecutive encounters.

- **Non-Resonant Transfers**: trajectories connecting two gravity assists occurring at different positions on the moon's orbit. They are also described through an N:M ratio, but the encounter geometry is not repeated at the same longitude. These transfers are further classified as IO or OI, depending on whether the spacecraft moves from an inbound to an outbound encounter condition, or vice versa.

- **COT Sequences [15]**: chained resonant-transfer sequences in which each flyby rotates the v∞ vector while preserving its magnitude and pump angle, thus changing only the crank angle κ. Each COT sequence is built to produce an overall crank-angle variation Δκ = π, switching the encounter condition from inbound to outbound or from outbound to inbound. Since intermediate crank-angle values different from 0 and π are allowed, these sequences are also useful to generate out-of-plane surface coverage during repeated flybys.

- **VILTs [16]**: powered transfers in which a tangential impulsive manoeuvre is performed after k1 spacecraft revolutions around the primary. The manoeuvre can occur either at the apocentre of the trajectory, defining an exterior VILT, or at the pericentre, defining an interior VILT. The notation adopted for these transfers is:

$$\{int\ or\ ext\} - N{:}M(k_1) - \{II, IO, OI\ or\ OO\} \quad (1)$$

where $N{:}M$ defines the resonance structure, k_1 identifies the number of spacecraft revolutions before the manoeuvre, and the final term specifies the initial and final encounter conditions.

With the exception of COT sequences, the motion is restricted to the equatorial plane. This modelling choice increases the number of admissible Non-Resonant transfers and VILTs, since extending them to a fully three-dimensional setting would force the initial and final encounters to lie on the line of nodes of the corresponding orbits. COT sequences are instead retained as a way to introduce out-of-plane flybys and improve surface coverage while keeping the design space computationally manageable.

The discretisation is performed using the V-Infinity Globe. For each moon in the planetary system, a grid of v∞ values is defined, corresponding to a set of concentric V-Infinity Globe levels. On each level, the relevant resonant transfers, non-resonant transfers, COT sequences, VILTs, and feasible unpowered flyby connections are computed and stored. Each point on the discretised globe therefore represents a possible encounter state, while each admissible transfer represents a possible transition between states.

The resulting information is stored in a structured database containing the v∞ levels, transfer families, and flyby connections available for each moon. Once initialized, this database provides a fully discretised design space for the graph-based optimizer, whose role is to search among precomputed building blocks and identify the sequence that best satisfies the selected cost function and mission constraints.

III. Single Moon Search Space Exploration through Graph-based Structures

For each moon in the system under analysis, the first optimization layer searches for admissible single-moon tours. These are obtained by chaining the previously defined building blocks, namely ballistic transfers, VILTs, COT sequences, and unpowered flybys. Ballistic transfers are used to modify the spacecraft encounter state with respect to the same moon without requiring any manoeuvre, while also allowing surface coverage to be accumulated during COT sequences and intermediate flybys. VILTs instead play a complementary role, since they enable transitions between different v∞ levels and therefore provide multiple possible entry and exit conditions for each single-moon phase. Since all the building blocks considered in this layer are phase-independent, they impose constraints only on the encounter geometry rather than on its absolute spatial orientation. As a result, the optimized single-moon solutions are not tied to a specific epoch and can later be used as reusable standalone transfers within a broader tour design process.

The single-moon optimization is formulated as a graph search problem over the predefined discretised design space. Each node represents a feasible encounter state and is defined as:

$$x = [moon, v\infty, \alpha, \kappa] \quad (2)$$

where $moon$ identifies the reference body, $v\infty$ is the hyperbolic excess velocity magnitude, α is the pump angle, and κ is the crank angle. The moon variable is retained in the node definition to ensure that the optimizer only connects states belonging to the same single-moon phase. The graph edges correspond to all admissible transfers departing from and arriving at the selected moon. At the beginning of the graph initialization, instantaneous unpowered flybys are also added as fictitious transfers between all physically patchable pairs of nodes. During this step, lower and upper bounds on the flyby hyperbola pericentre altitude are enforced, and all gravity assists violating these constraints are discarded.

For each stored COT sequence, which involves intermediate flybys, the associated surface coverage is also evaluated. A maximum working altitude is defined, and each moon's surface is discretised through a spherical Voronoi diagram. The zones intersected by the hyperbolic ground track below the selected altitude threshold are counted as covered, allowing the scientific return of each transfer to be included directly in the optimization process. Once the graph has been initialized, a scalar cost is assigned to each edge by combining surface coverage, ΔV, and ToF. The cost is defined as a weighted average, with normalized weights satisfying $w_{cov} + w_{\Delta V} + w_{ToF} = 1$:

$$c = [w_{cov}(1 - cov) + w_{\Delta V}\, \Delta V + w_{ToF}\, ToF] \,/\, [w_{cov} + w_{\Delta V} + w_{ToF}] \quad (3)$$

where cov is the normalized coverage contribution of the edge. After each edge has been assigned its cost, a heap-based Dijkstra algorithm is used to explore the graph and retrieve the globally optimal path from each possible departure node. The corresponding performance parameters are then evaluated, and only the non-dominated single-moon solutions are retained according to a weights-driven priority criterion.

It is worth highlighting the versatility of this approach. In this case, once every optimal solution departing from and arriving at each feasible encounter state is computed, and only non-dominated solution are retained. In other words, Dijkstra's algorithm allows to retrieve the set of all the possible non dominated sequences in terms of the chosen edge weighting functions for the considered design space. This set of trajectories can be then used at will during the mission design process, for example by retrieving feasible optimal trajectories given desired departure and arrival values of pump angle and v∞ or by selecting pre-computed sequences according to further mission constraints.

IV. SINGLE MOON RESULTS

The single-moon algorithm presented in the previous section has been tested on multiple case studies in the Saturnian system, involving different weighting in the cost function. For all the case studies, a finite number of predefined resonances already used in Enceladus tour design is considered and reported in Table 1 [16]. A significant test case is an almost purely coverage-driven tour ($w_{cov} = 0.9$, $w_{\Delta V} = 0.1$, $w_{ToF} = 0$), whose results are presented hereafter.

Several solutions are found per each moon, all of them in less than 20 minutes, computed on a laptop with an Intel Core i7 13700H processor and a 16 GB RAM. The solution front computed for tours at Rhea is presented in Figure 2, where each solution is represented in a different colour depending on its final v∞ value. This front encompasses 49652 non-dominated solutions, computed in 17 min 18 s. As it can be noted, no direct correlation between ΔV and coverage is present. This can be promptly understood by looking at the way in which, in this case, out-of-plane coverage is achieved: COT sequences are patterns of chained resonant transfers, thus ballistic by their very nature. On the other hand, a shape similar to that of a Pareto front can be noticed in the coverage-*ToF* plot, since COT sequences strongly increase both of them.

Table 1: List of selected resonances.

Moon	Resonances
Titan	3:1, 2:1, 1:1
Rhea	1:1, 13:7, 9:7, 4:5, 5:3, 3:1, 7:6, 3:2, 7:5, 4:3, 5:4, 6:5, 15:14, 14:15, 2:2, 3:3, 4:4, 6:7, 2:1, 5:3, 8:5, 7:4, 15:8, 17:8, 9:8, 8:9, 8:7, 7:8, 10:9, 9:10, 11:10, 10:11, 12:11, 11:12, 13:12, 12:13
Dione	1:1, 4:3, 9:7, 5:4, 6:5, 7:6, 8:7, 9:8, 10:9, 11:10, 12:11, 13:12, 19:18, 18:19, 14:15, 12:13, 11:12, 10:11, 9:10, 8:9, 7:8, 6:7, 3:3, 4:4, 5:5, 27:26, 26:27, 26:25, 25:26, 25:24, 24:25
Tethys	1:1, 11:9, 6:5, 7:6, 8:7, 9:8, 10:9, 11:10, 12:11, 13:12, 14:13, 15:14, 19:18, 25:24, 35:34, 34:35, 24:25, 18:19, 14:15, 13:14, 10:11, 9:10, 7:8, 13:15, 4:4, 5:5, 6:6, 34:33, 33:32, 33:32, 32:33, 32:31, 31:32, 31:30, 30:31, 30:29, 29:30, 29:28, 28:29, 28:27, 27:28
Enceladus	1:1, 7:6, 20:17, 15:13, 8:7, 17:15, 9:8, 19:17, 10:9, 21:19, 11:10, 12:11, 13:12, 14:13, 15:14, 16:15, 19:18, 24:23, 17:16, 21:20, 13:11, 22:19, 15:13, 25:22, 18:17

One of the best solutions is reported in Figure 3, showcasing a tour at Rhea reaching full surface coverage in 520.5 days, with only 12.5 m/s of total ΔV. The sequence of transfers followed by the spacecraft includes multiple COT sequences that increase the coverage, resonances to change the pump angle, and non-resonant transfers to switch the encounter condition in a single shot. In this case, the COT sequences that are used are 3:2, 4:3 and 1:1, which alternate with 7:5, 10:9 and 10:11 resonances and OI 9:7 and OI 12:13 non-resonant transfers.

The final transfer is an int-4:5(4)-OI VILT, that links the initial and final v∞ levels in the cheapest way possible. Naturally, ballistic sequences are also found, but in order to present a complete scenario, a solution with different levels is presented.

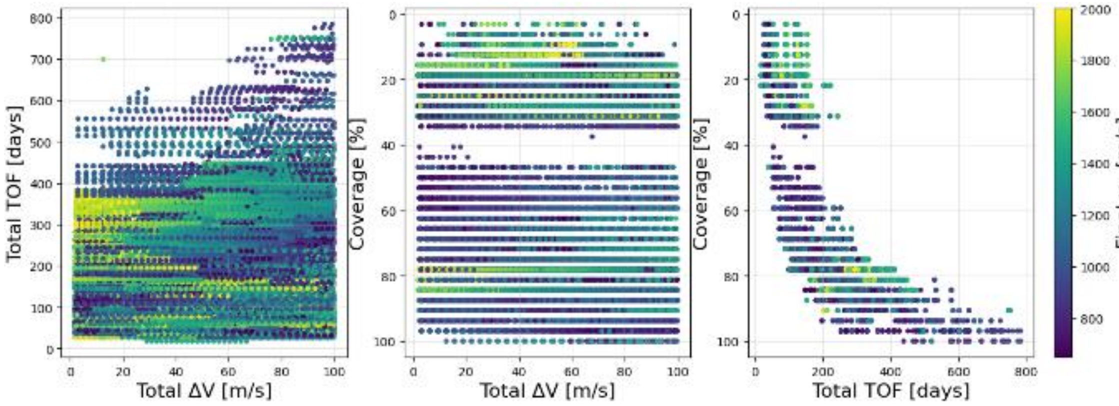

Figure 2: Solution set for tours at Rhea ($w_{cov} = 0.9, w_{\Delta V} = 0.1, w_{ToF} = 0$).

All the transfers are linked by natural flybys, whose pericentre altitude stays inside a predefined acceptable range of values, which can be tuned to fulfil scientific requirements. The ground tracks of the tour over Rhea's surface are reported in Figure 4. The colour of the track indicates the altitude of the spacecraft over the moon's surface: moving from the asymptotes of the hyperbola to the lower altitude region, the trajectory goes from a dark purple to yellow, until eventually reaching the pericentre, represented with a red dot.

The framework has been tested also considering non-zero weights for the three objectives ($w_{cov} = 0.4$, $w_{\Delta V} = 0.3$, $w_{ToF} = 0.3$). The results is reported in Figure 5. In this case the number of non-dominated solutions is 49690, computed in 16 min 59 s. As it can be seen, the results of this case are very similar to the coverage-driven ones. Just like in the previous case, in fact, no correlation between *ΔV* and *ToF* can be seen, while the trade-off options are present in the coverage-*ToF* plot.

V. Inter Moon Search Space Exploration through Graph-Based Structures

Once the non-dominated single-moon solutions have been computed, they are passed to a second, preliminary optimization layer aimed at investigating the possibility of assembling them into multi-moon sequences through inter-moon Lambert arcs. Differently from the single-moon case, this external layer is time-dependent, because transfers between different moons depend on their relative orbital positions at the departure epoch. For this reason, the node definition is extended by including the epoch at which the state is reached:

$$x = [moon, v\infty, \alpha, \kappa, et] \quad (4)$$

where et denotes the encounter epoch. For each departure epoch, all admissible departure nodes at Titan are initialized, and the external graph construction is started.

Because of the time dependency introduced by the inter-moon connections, the complete graph is not generated a priori. Instead, an Implicit Graph Uniform Cost Search algorithm is employed, so that successor nodes are generated at runtime. During the expansion of each node, all states reachable through an instantaneous unpowered flyby are first considered. Then, inter-moon Lambert arcs are computed to connect the current state to feasible states at other moons. For each Lambert

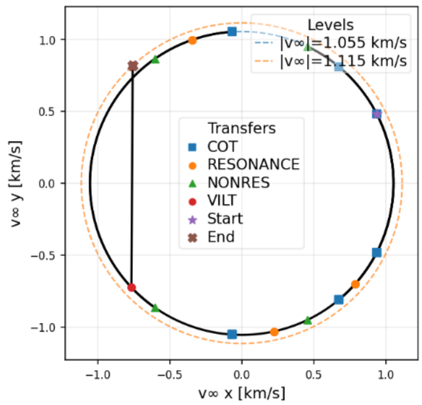

Figure 3: Tour at Rhea on the 2D projection of its V-Infinity Globe.

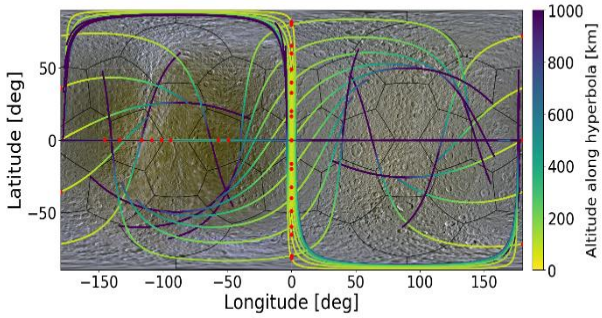

Figure 4: Ground tracks of the tour at Rhea.

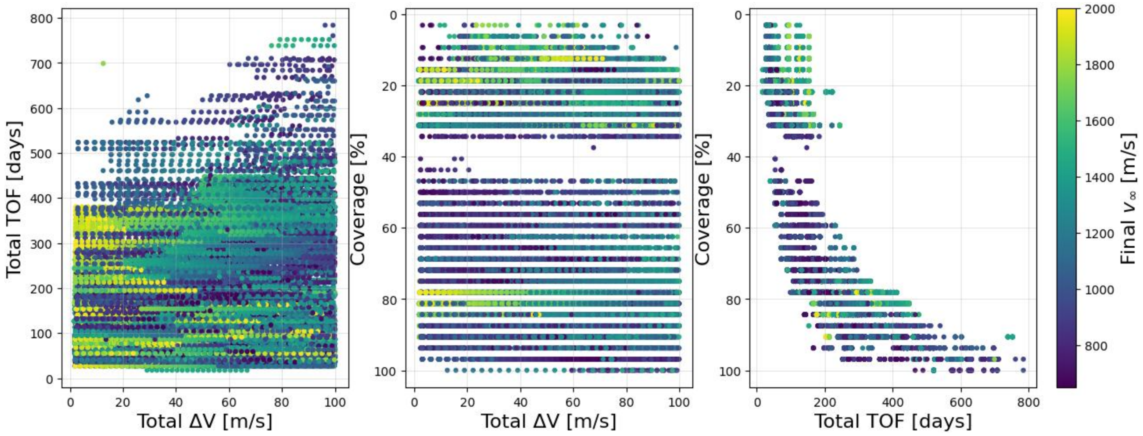

Figure 5: Solution set for tours at Rhea ($w_{cov} = 0.4, w_{\Delta V} = 0.3, w_{ToF} = 0.3$).

transfer, a one-dimensional refinement of the *ToF* is applied using finite-difference sensitivities of the departure and arrival v∞ magnitudes with respect to the *ToF*. This correction aims to better match the required v∞ levels at both ends of the transfer and to avoid introducing excessively costly patching manoeuvres.

The node expansion continues until one of the imposed stopping criteria is reached. In particular, paths are discarded when upper bounds on cumulative *ΔV* or total *ToF* are exceeded. In addition, dominance pruning is applied: if another sequence reaches the same aggregated state with a lower scalar cost, the more expensive sequence is discarded. The scalar cost used in this external layer follows the same structure adopted for the single-moon optimization, allowing the search to consistently balance *ΔV*, *ToF*, and coverage-related objectives. This second layer is therefore treated as a preliminary extension of the main single-moon framework, providing an initial assessment of whether the optimized single-moon phases can be patched into feasible multi-moon tours, while leaving the refinement of the inter-moon connection strategy to future developments.

VI. Inter Moon Results

The inter-moon algorithm has been tested in the Saturnian system, taking as input the solution sets of the single-moon search. Since in this case the initial epoch is part of the design variables, a departure window is defined over one synodic period of the outermost moons considered in the system, Titan and Rhea, corresponding to approximately 6.3 days, and is discretised with a 6-hour step. The results, 40195 solutions computed in 2 h 29 min, are shown in Figure 6, distributed by their departure epochs. For each departure epoch, the red dot indicates the best solution, in this case in terms of total obtained coverage of the system of moons. As it can be seen, the departure epoch strongly influences the outcome of the tour, since the spatial disposition of the moons varies and

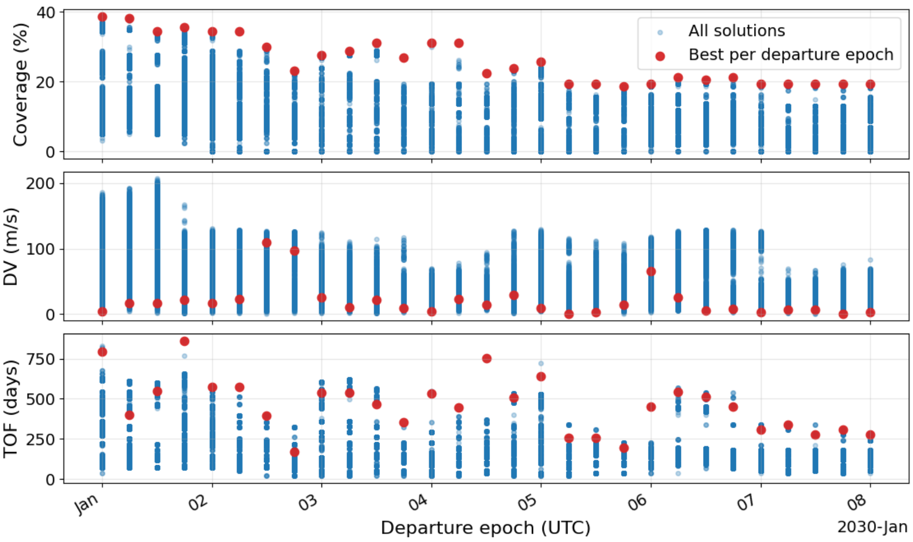

Figure 6: Solutions of the inter-moon phase.

changes the possibilities of transfers from one to the other. Moreover, no solution can be found that achieves more than 40% total coverage. This is due to the fact that all the tours stop after reaching Rhea. No Lambert arcs, with the currently employed approximation and departure window, are found that match the initial and final conditions to advance through Dione and proceed.
However, the most promising solution among the ones computed shows a 38.75% coverage, obtained in 794.4 days with 4.1 m/s of total ΔV. It important to notice that the coverage percentage refers to the whole moon system, but it is composed of a 71.88% coverage of Titan and a 100% coverage of Rhea, meaning that 85.94% of the ensemble of the visited moons is successfully covered.

Due to the limited results, additional tests have been performed by bypassing the Lambert-arc generation and imposing departure and arrival states from a reference tour [18] showed that complete sequences from Titan to Enceladus with overall coverage above 60% can be constructed. For example, 62.5% coverage of the whole moons system has been reached in 11.72 years, with 138.75 m/s of ΔV.

VII. CONCLUSIONS AND FUTURE WORK

This work presented a graph-based pipeline for the automated generation of constrained Moon Tour sequences, with the main contribution lying in the construction and optimization of single-moon flyby phases. The results obtained at this level confirm the validity of the adopted strategy: the V-Infinity Globe discretisation provides a compact but expressive representation of the design space, allowing resonant transfers, non-resonant transfers, COT sequences, VILTs, and unpowered flybys to be combined efficiently within a unified graph structure. The resulting single-moon solutions are able to maximize surface coverage while keeping ΔV and *ToF* under control, and the computational burden remains compatible with early-phase mission analysis, since relevant sets of transfers can be generated in minutes on a standard laptop. This confirms that graph structures and graph-search algorithms are well suited to automate the selection of transfer sequences under science- and mission-related constraints, especially when the problem is restricted to phase-independent single-moon dynamics.

The preliminary inter-moon extension showed more critical limitations. Optimized single-moon phases are treated as standalone-transfers and connected through Lambert arcs in a time-dependent external graph, but the resulting sequences did not cover the full moon system. This mainly highlights weaknesses in the inter-moon patching strategy rather than in the single-moon framework. Strict dominance pruning may discard useful intermediate solutions, while the first-order ToF correction applied to Lambert arcs can fail under nonlinear v_∞-matching constraints, even when a valid connection may exist. A wider or more finely discretised departure window could also improve the exploration of feasible inter-moon opportunities. Nevertheless, tests bypassing Lambert arc computation suggest that the underlying discretised design space and single-moon solutions contain promising trajectory options, and that the main bottleneck is the robustness of the inter-moon connection layer rather than the graph-based optimization concept itself.

Future work should therefore focus on improving the inter-moon patching strategy, for instance by replacing the current one-dimensional Lambert *ToF* correction with a more robust local optimization, relaxing the v_∞ matching constraints, retaining a richer set of non-dominated single-moon candidates, and testing less aggressive dominance-pruning policies. Additional developments should also investigate the sensitivity of the results to the discretisation parameters, the cost-function weights, and the departure-window resolution. Finally, once more robust inter-moon connections are obtained, the generated tours should be refined using full-ephemeris and higher-fidelity dynamical models, so that the proposed framework can provide reliable initial guesses for subsequent continuous trajectory optimization.

VIII. REFERENCES

[1] C. C. Porco, P. Helfenstein, P. C. Thomas, A. P. Ingersoll, J. Wisdom, R. West, G. Neukum, T. Denk, R. Wagner, T. Roatsch, et al., “Cassini observes the active south pole of Enceladus”, Science, vol. 311, no. 5766, pp. 1393–1401, 2006.
[2] T. M. Becker, M. Yu. Zolotov, M. S. Gudipati, J. M. Soderblom, M. A. McGrath, B. L. Henderson, M. M. Hedman, M. Choukroun, R. N. Clark, C. Chivers, et al., “Exploring the composition of Europa with the upcoming Europa Clipper mission”, Space Science Reviews, vol. 220, no. 5, article 49, 2024.
[3] N. J. Strange, R. P. Russell, and B. Buffington, “Mapping the V-Infinity Globe”, AAS Paper 07-277, 2007.
[4] S. Campagnola and R. P. Russell, “Endgame problem part 2: multibody technique and the Tisserand-Poincaré graph”, Journal of Guidance, Control, and Dynamics, vol. 33, no. 2, pp. 476–486, 2010.
[5] S. Campagnola, P. Skerritt, and R. P. Russell, “Flybys in the planar, circular, restricted, three-body problem”, Celestial Mechanics and Dynamical Astronomy, vol. 113, no. 3, pp. 343–368, 2012.

[6] N. J. Strange, “Analytical Methods for Gravity-Assist Tour Design”, Ph.D. dissertation, Purdue University, 2016.

[7] B. Buffington, N. J. Strange, and S. Campagnola, “Global moon coverage via hyperbolic flybys”, 23rd International Symposium on Space Flight Dynamics, 2012.

[8] S. Campagnola and R. P. Russell, “Endgame problem part 1: V-infinity-leveraging technique and the leveraging graph”, Journal of Guidance, Control, and Dynamics, vol. 33, no. 2, pp. 463–475, 2010.

[9] S. Campagnola, A. Boutonnet, J. Schoenmaekers, D. J. Grebow, A. E. Petropoulos, and R. P. Russell, “Tisserand-leveraging transfers”, Journal of Guidance, Control, and Dynamics, vol. 37, no. 4, pp. 1202–1210, 2014.

[10] G. Colasurdo, A. Zavoli, A. Longo, L. Casalino, and F. Simeoni, “Tour of Jupiter Galilean moons: Winning solution of GTOC6”, Acta Astronautica, vol. 102, pp. 190–199, 2014.

[11] A. Marrazza and V. Levi, “Trajectory optimization for Jovian moon exploration using single and multi-objective beam search”, IAF Astrodynamics Symposium, Milan, Italy, pp. 1308–1323, 2024.

[12] F. Maccari and M. Lavagna, “Multi-objective graph search for automated planetary moon tour design”, AIAA SCITECH 2026 Forum, paper 1460, 2026.

[13] D. H. Ellison and C. J. Scott, “Europa Clipper mission analysis: a flexible graph-based search automation for gravity-assist trajectory design”, Astrodynamics Specialist Conference, AAS 24-425, 2024.

[14] S. M. LaValle, Planning Algorithms, Cambridge University Press, 2006.

[15] B. Buffington, N. J. Strange, and S. Campagnola, “Global moon coverage via hyperbolic flybys”. 23rd International Symposium on Space Flight Dynamics, page 20, 2012.

[16] N. J. Strange, S. Campagnola, and R. P. Russell, “Leveraging flybys of low mass moons to enable an enceladus orbiter”, Advances in the Astronautical Sciences, 135(3):2207–2225, 2009.

[17] A. Bellome, J. P. Sanchez, J. C. Garcia Mateas, A. Boutonnet, W. Martens, M. Sciarra, D. Morante, P. Hermosin, “Multi-objective dynamic programming for saturn moon tours design”, 29th International Symposium on Space Flight Dynamics, 2024.

[18] Y. Takubo, D. Landau, and B. Anderson, “Automated tour design in the saturnian system”, Celestial Mechanics and Dynamical Astronomy, 136(1):8, 2024.